PNAS RESEARCH ARTICLE | PSYCHOLOGICAL AND COGNITIVE SCIENCES

Cortisol awakening response prompts dynamic reconfiguration of brain networks in emotional and executive functioning

Yimeng Zeng[a,b,c], Bingsen Xiong[d], Hongyao Gao[b,c], Chao Liu[b,c], Changming Chen[e], Jianhui Wu[f], and Shaozheng Qin[b,c,g,1]

Affiliations are included on p. 10.

Edited by Marcus Raichle, Washington University in St Louis School of Medicine, St. Louis, MO; received March 22, 2024; accepted September 20, 2024

Emotion and cognition involve an intricate crosstalk of neural and endocrine systems that support dynamic reallocation of neural resources and optimal adaptation for upcoming challenges, an active process analogous to allostasis. As a hallmark of human endocrine activity, the cortisol awakening response (CAR) is recognized to play a critical role in proactively modulating emotional and executive functions. Yet, the underlying mechanisms of such proactive effects remain elusive. By leveraging pharmacological neuroimaging and hidden Markov modeling of brain state dynamics, we show that the CAR proactively modulates rapid spatiotemporal reconfigurations (state) of large-scale brain networks involved in emotional and executive functions. Behaviorally, suppression of CAR proactively impaired performance of emotional discrimination but not working memory (WM), while individuals with higher CAR exhibited better performance for both emotional and WM tasks. Neuronally, suppression of CAR led to a decrease in fractional occupancy and mean lifetime of task-related brain states dominant to emotional and WM processing. Further information-theoretic analyses on sequence complexity of state transitions revealed that a suppressed or lower CAR led to higher transition complexity among states primarily anchored in visual-sensory and salience networks during emotional task. Conversely, an opposite pattern of transition complexity was observed among states anchored in executive control and visuospatial networks during WM, indicating that CAR distinctly modulates neural resources allocated to emotional and WM processing. Our findings establish a causal link of CAR with brain network dynamics across emotional and executive functions, suggesting a neuroendocrine account for CAR proactive effects on human emotion and cognition.

cortisol | dynamic networks | emotion | executive function | hidden Markov model

Significance

Human emotion and cognition involve complex neural and endocrine interactions, allowing neural resource allocation to support optimal adaptability and flexibility for changing demands. Our understanding of this allostatic process remains limited. The cortisol awakening response (CAR) is a key mediator of allostasis, influencing emotional and cognitive functions via brain networks. Little, however, is known about how CAR-induced neuroendocrine crosstalk supports dynamic organization of functional brain networks. Using pharmacological neuroimaging and hidden Markov modeling, we show that CAR proactively fosters emotional discrimination and working memory, by modulating task-specific brain state occupancy and network dynamic reconfigurations reflecting resource allocation. Our findings provide insights into the neuroendocrine mechanisms underlying CAR proactive modulations on brain network dynamics and resource allocation across emotion and cognition.

For centuries, scientists have sought to unravel how the brain and endocrinal signals work in concert to support ever-changing cognitive and environmental demands. In theory, to sustain a dynamic equilibrium between internal milieu and external challenges, the brain and endocrinal signals actively engage in allocation of neural resources to prepare for the upcoming challenges (1, 2). Such active process has been conceptualized as "allostasis" and is believed to serve as one key principle of how neural and endocrinal signals interplay to support nuanced emotional and executive functions, though the underlying mechanisms remain largely elusive. Among endocrinal signals, the stress hormone cortisol plays a critical role in mobilizing energy supply for brain, cognition, and emotion (1, 3, 4). The cortisol awakening response (CAR), in particular, as a natural rise of cortisol through activation of the hypothalamus–pituitary–adrenal (HPA) axis within 30 to 45 min after morning awakening, is superimposed upon the circadian rhythm of cortisol secretion and is more than the mere release of cortisol (5–7). The CAR has been thought to support anticipation of a day's most reliable stressor—waking up, mobilizing the energy to daily activities (8–10) and proactively modulates human emotion and cognition (11–13). Such proactive effects are reminiscent of a potential mediator of allostasis (1, 14). Although the CAR proactive effects are well documented at a behavioral level, our understanding of the underlying neurobiological mechanisms still remains in its infancy.

Psychological and neurobiological theories attempt to account for the CAR proactive effects on human cognition and emotion. The prospective view suggests a CAR-induced preparation function for upcoming workload and challenges, via activation of one's prospective memory representations and appraisal of anticipating the demands for the day ahead (8, 15). The neurobiological models of cortisol suggest that CAR upon morning awakening can set up a tonic tone as background activity to mobilize metabolism and energy supply for the brain and body, through intricate expression of mineralocorticoid (MRs) and glucocorticoid receptors (GRs) that act on neuronal excitability of brain networks (16, 17). While the MR-mediated nongenomic actions can initiate rapid changes

The authors declare no competing interest.

This article is a PNAS Direct Submission.

Copyright © 2024 the Author(s). Published by PNAS. This article is distributed under Creative Commons Attribution-NonCommercial-NoDerivatives License 4.0 (CC BY-NC-ND).

[1]To whom correspondence may be addressed. Email: szqin@bnu.edu.cn.

This article contains supporting information online at https://www.pnas.org/lookup/suppl/doi:10.1073/pnas.2405850121/-/DCSupplemental.

Published December 16, 2024.

Downloaded from https://www.pnas.org by HEFEI UNIVERSITY OF TECHNOLOGY on December 16, 2024 from IP address 114.213.251.57.

that activate neural circuits in response to acute stress and emotional arousal, the relatively slower genomic GR-mediated actions come to play later to promote adaptation and memory consolidation throughout the day (16, 18–20). Recent neuroimaging studies have demonstrated that CAR-induced tonic activity may improve neural efficiency involving amygdala-prefrontal systems in emotional processing (12) and prefrontal–hippocampal interactions underlying executive functions even 6 h later in the afternoon (13). Beyond separate systems, nuanced emotional and executive functions require dynamic (re)configuration of large-scale brain networks to support optimal adaptation and behavioral flexibility, as illuminated by recent advances in cognitive and network neuroscience (21–24). Yet, little is known about how CAR could leverage its proactive modulation on brain network dynamics across emotional and executive functions.

One fundamental question regarding CAR is how its tonic activity upon awakening is converted into proactive modulations on emotion and cognition hours later, while still being flexible enough to impact diverse task demands. Based on neurobiological models of cortisol and catecholamines, it is conceivable that CAR's proactive effects on brain functioning are likely mediated through an interplay between CAR-initiated tonic background activity and task-dependent phasic catecholaminergic actions that modulate neuronal excitability and inhibition of emotional and executive brain networks (25–28). For instance, activity in emotion-related sensory and limbic structures (including amygdala and thalamus) can be modulated by cortisol levels and stimulus-induced norepinephrine (29–32) to prompt rapid configurations of stimulus-sensitive sensory and salience networks that are critical for vigilance and emotion processing (33). Meanwhile, interactions between cortisol and phasic catecholaminergic signals that project to the prefrontal cortex and related circuits can improve neural efficiency in working memory (WM), likely via optimizing dynamic organization of executive control networks for resource allocation (13, 28, 34, 35). Together, we hypothesize that CAR would proactively optimize human emotional and executive functions, likely via acting on task-dependent brain network activity states involved in these functions.

In the neurobiology of allostasis (1, 36), intricate interplay of brain systems and endocrinal signals has long been thought to support allocation of neural resources for regulating energy supply and enabling behavioral flexibility and adaptation for changing challenges (37–39). For example, stimulus-induced catecholaminergic signals are proved crucial for prompting wide-spread brain network reconfigurations and shifting neural gain for cognitive demands (40, 41), therefore modulating resource allocation among network modules to optimize cognitive and affective functioning (29, 38, 40, 42). As a potential mediator, one may thus conjecture that CAR-initiated tonic activity in the morning could leverage a similar mechanism of resource allocation, through interplay with task-induced neurotransmitters to modulate emotion and cognition. Recent computational studies have linked neural resource allocation modulated by neurotransmitters to dynamic brain state transitions (43) or alteration of energy landscape (38). Dynamical network modeling such as hidden Markov modeling (HMM) offers useful approach to probe time-resolved functional (re)configuration of brain networks under diverse tasks (44–46). Based on Viterbi decoded sequence, brain state dynamics can be quantified by fractional occupancy, mean lifetime, and system-level state transitions, providing an ideal approach to probe CAR's proactive effects on brain network dynamics and neural resource allocation (38). According to above CAR-mediated preparation function and task-induced catecholaminergic modulations, we further hypothesize that CAR would have distinct modulations on system-level state transitions anchored onto task-specific brain networks across emotional and WM processing, reflecting flexible neural resources allocated to these processes.

Here, we test above hypotheses by combining a double-blinded pharmacological manipulation (Cohort 1) dedicated to the CAR with salivary samples across three consecutive days, in conjunction with a multitask paradigm. An independent Cohort 2 with natural assessment of the CAR and similar task designs was included to further validate the CAR proactive effects from pharmacological cohort. As shown in Fig. 1, participants in Cohort 1 received either 0.5-mg dexamethasone (DXM) or placebo (vitamin C) on Day 1 night at 20:00 to suppress CAR in the next morning. Saliva samples were collected at 15 time points over three consecutive days to measure cortisol levels. On Day 2 afternoon, participants underwent functional MRI (fMRI) to perform resting state, emotion matching, and WM tasks, when cortisol levels were no different in afternoon between groups. Based on data from Cohorts 1 and 2, we first investigated the proactive effects of CAR on emotional and WM task performance. We then implemented HMM to probe dynamical organization of large-scale functional brain networks and investigated how the CAR modulates brain state dynamics under emotional and WM tasks. Finally, we implemented information theory-based algorithms to compute the sequence complexity of state transitions (namely, transition complexity) and examined how CAR modulates neural resource reallocation across emotional and WM tasks.

Results

Effectiveness of CAR Suppression and Its Proactive Effects on Behavioral Performance. We conducted the pharmacological manipulations at 20:00 on Day 1 night to ensure that the CAR was suppressed in the next morning, while cortisol levels kept no difference between groups during fMRI scanning in the afternoon (Fig. 1 *A* and *B*). This pharmacological timing was identified by one pilot experiment (*SI Appendix*, Fig. S1). To verify the effectiveness of CAR suppression, we compared cortisol levels between two groups from Day 1 to Day 3, by conducting a 2 (Group: DXM vs. Placebo)-by-15 (Time: 15 samples) repeated-measure ANOVA. This analysis revealed a significant main effect of Group ($F_{1,59}$ = 19.0, $P < 0.001$) and Group-by-Time interaction effect ($F_{14,826}$= 19.4, $P < 0.001$). Post hoc tests revealed a blunted CAR in the morning on Day 2 as shown at 7:00, 7:15, 7:30, and 8:00 AM after awakening in the DXM group (All Ps < 0.001), but no group difference in cortisol levels was observed before and after fMRI scanning (All Ps > 0.24). We further examined group differences in two measures of CAR, including area under curve with respect to increase at 7:00 AM (AUCi) and to ground zero (AUCg), reflecting a dynamic (state-like) rise and an overall cortisol secretion within 1-h postawakening, respectively (*Methods*). Two sample t tests revealed significantly lower AUCi (t_{59} = −2.10, P = 0.04) and AUCg (t_{59}= −9.61, $P < 10^{-13}$) in the DXM group than Placebo (*SI Appendix*, Fig. S2), further validating the effectiveness of CAR suppression.

We then investigated how the CAR proactively modulates subsequent behavioral performance in emotional and WM tasks in the afternoon (*Methods*). After excluding outliers, a 2 (Group: DXM vs. Placebo)-by-2 (Emotion vs. Neutral) ANOVA was conducted for accuracy of emotion discrimination task. As shown in Fig. 1*C*, this analysis revealed significant main effects of Group ($F_{1,57}$ = 9.01, P = 0.004) and Emotion condition ($F_{1,57}$ = −5.24, $P < 0.001$), as well as their interaction effect ($F_{1,57}$ = 6.88, P = 0.011). Post hoc t tests revealed higher accuracy of emotion condition in Placebo than DXM group (t_{57} = 2.97, $P < 0.01$), but

Downloaded from https://www.pnas.org by HEFEI UNIVERSITY OF TECHNOLOGY on December 16, 2024 from IP address 114.213.251.57.

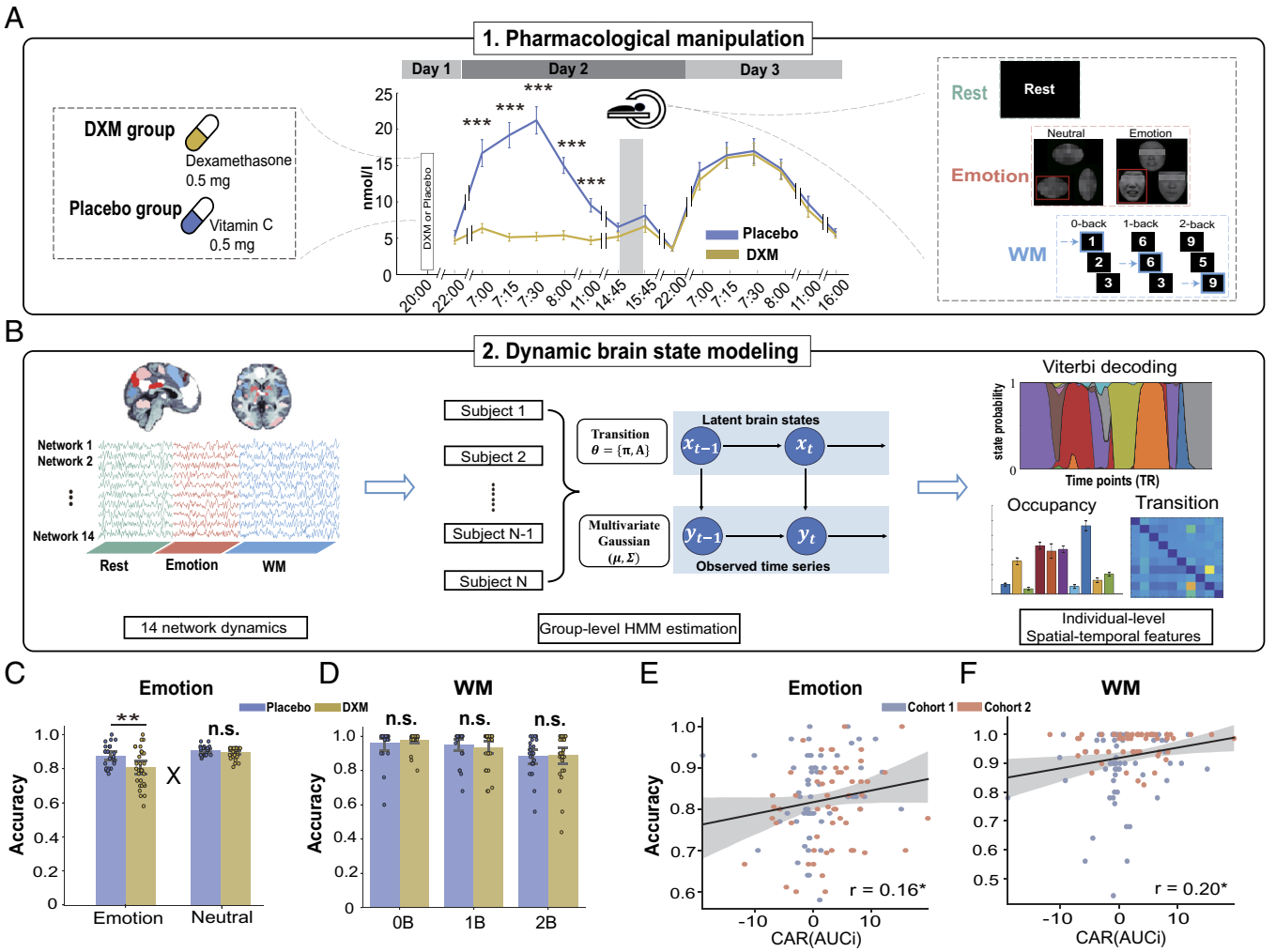

Fig. 1. Experimental design with pharmacological manipulations, fMRI tasks, the effectiveness of CAR suppression, and behavioral performance. (*A*) On Day 1 night, participants were administered either 0.5 mg of DXM or the same dosage of placebo. On Day 2 afternoon, participants completed three consecutive tasks including rest, emotion matching, and N-back WM. A total of 15 time-stamped participants' saliva samples were collected throughout 3 d to measure CAR levels. (*B*) BOLD time series during fMRI scanning in the afternnon of Day 2 were extracted as 14 prior-defined brain networks of interest. Hidden Markov model was implemented to estimate network dynamics across three tasks. (*C* and *D*) Bar graphs depict accuracy of emotional discrimination task and WM under each task condition and group. (*E* and *F*) Scatterplots depict significant positive correlations between AUCi measure of CAR and accuracy in emotional and WM 2-back conditions. Notes: n.s., nonsignificance; *P < 0.05, **P < 0.01.

no difference in neutral condition (t_{57} = 1.24, P = 0.22). Parallel analysis for WM accuracy revealed significant main effect of WM loads ($F_{2,108}$ = 20.47, P < 0.001), but neither Group ($F_{1,54}$ = 0.04, P > 0.80) nor Group-by-WM interaction effect ($F_{2,108}$ = 0.99, P = 0.38) (Fig. 1*D*). Given a similar pattern of behavioral data observed in Cohort 2 (*SI Appendix*, Fig. S5), we thus combined data from two cohorts for further correlation analyses. Permutation tests revealed significantly positive correlations of CAR (i.e., AUCi) with accuracy in both emotional (r = 0.16, P = 0.039) and WM 2-back conditions (r = 0.20, P = 0.018). Notably, Spearman correlations are also significant (Ps < 0.04). Together, these results indicate the effectiveness of CAR suppression by our pharmacological manipulation, an impairment in emotional discrimination task in general, and relatively poorer performance in both emotional and WM tasks in individuals with lower CAR.

CAR Proactive Effects on Brain State Occupancy during Emotional and Executive Functions. To detect brain network dynamics across different tasks, we implemented HMM for BOLD time series of 14 brain networks during Rest, Emotion, and WM tasks collapsing across Placebo and DXM groups. Detail procedures and verification of selecting number of states are provided in *Methods* and *SI Appendix*, Fig. S6. As shown in Fig. 2*A*, modeling outputs with inferred 10 states featured by distinct network configurations which capture rich brain network dynamics across three tasks (see *SI Appendix*, Fig. S7 for the rest states). Based on Viterbi-decoded state sequence, we calculated fractional occupancy (Fig. 2*B*) and mean lifetime (*SI Appendix*, Fig. S8) of each brain state for Rest, Emotion, and WM tasks. We found significantly higher fractional occupancy of State 2 (S2) and State 10 (S10) during Rest, State 1 (S1), and State 8 (S8) during Emotion task as well as State 4 (S4) and State 5 (S5) during WM task, as compared to the others (*all Ps* < 0.05 FDR corrected, Fig. 2*B*). From a holistic view, we implemented t-SNE algorithm to visualize the distribution of states' fractional occupancy under Rest, Emotion, and WM tasks, and the low-dimensional clustering result further validates task-dependent states distributions (Fig. 2*C*). Notably, we observed similar brain state dynamics across Rest, Emotion, and WM tasks in Cohort 2 (*SI Appendix*, Fig. S9).

To further test our hypothesis of how CAR proactively modulates brain state dynamics across emotional and WM tasks, we compared fractional occupancy and mean lifetime of brain states dominant to these two tasks between Placebo and DXM groups. We first conducted a knee-point analysis to identify brain states

Downloaded from https://www.pnas.org by HEFEI UNIVERSITY OF TECHNOLOGY on December 16, 2024 from IP address 114.213.251.57.

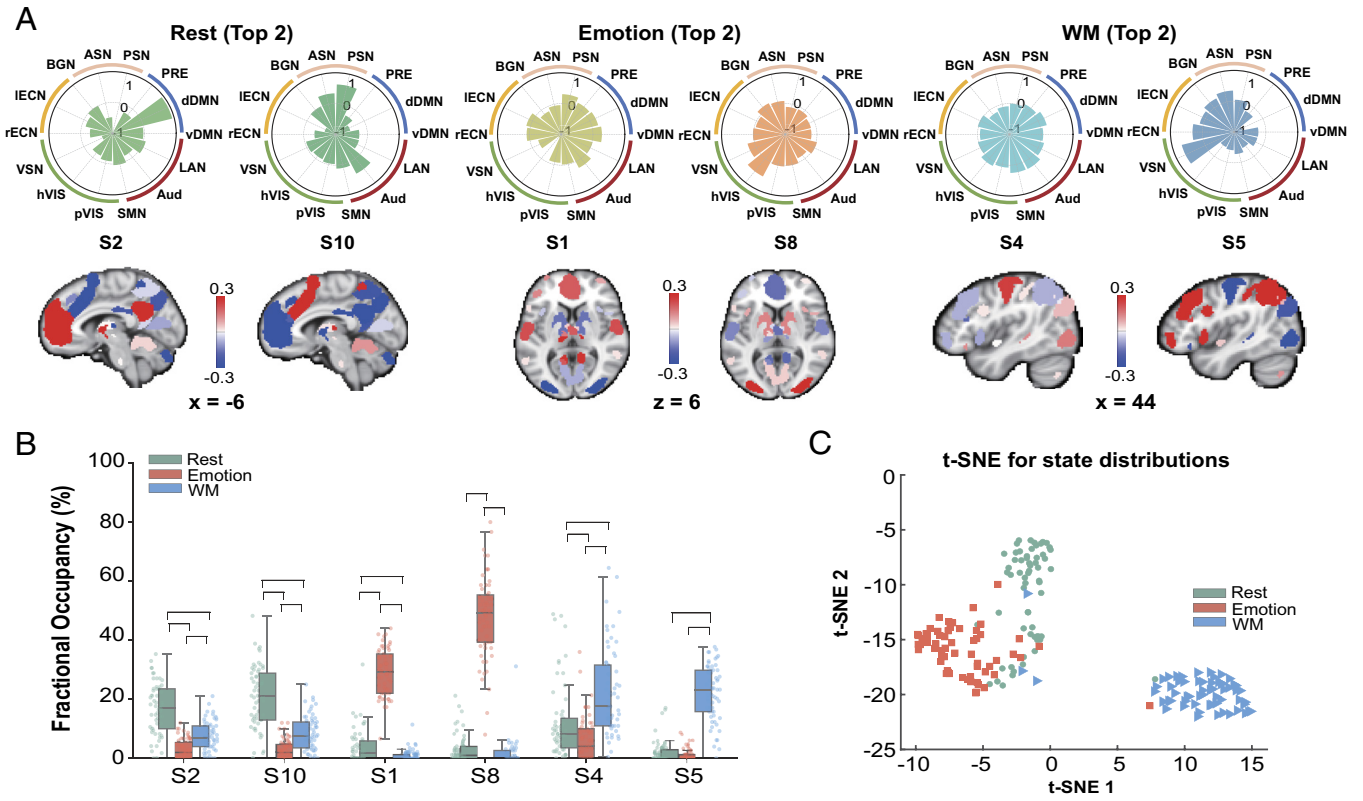

Fig. 2. Brain network configuration patterns of each state across Rest, Emotion, and WM tasks. (*A*) Polar graphs represent each inferred brain state featured by their relative load of 14 canonical networks with the top two occupied states for each task shown for visualization purpose. The value of each bar indicates the relative activity magnitude compared with the average activity inferred from HMM. The order of brain networks in the polar graphs is organized by their functional specialization. Each state's magnitudes are overlaid in Montreal Neurological Institute (MNI) space. (*B*) Relative occupancy rate of these brain states during Rest, Emotion, and WM, respectively. Horizontal lines represent significant differences in fractional occupancy ($P < 0.05$, FDR corrected) among three tasks for each state. (*C*) t-SNE embedding for distributions of fractional occupancy from all states for Rest, Emotion, and WM tasks. Notes: Sensorimotor Network (SMN), Precuneus Network (PRE), Left, and Right Executive Control Networks (lECN, rECN), Anterior, and Posterior Salience Networks (ASN, PSN), Visuospatial Network (VSN), Dorsal and Ventral Default Mode Networks (dDMN and vDMN), Primary and High Visual Networks (pVIS, hVIS), Auditory Network (AUD), Language Network (LAN).

that most commonly occurred under each task (*SI Appendix*, Fig. S10). This revealed a set of dominant states for Rest, Emotion, and WM tasks separately (Fig. 3*A*). We then focused on the dominant brain states under each task to address our central question at issue for the emotional and 2-back conditions, with the top two occupied states shown in Fig. 3 for visualization purpose. Among dominant states for emotional task, we identified only state S8's occupancy showing a positive correlation with emotional discrimination accuracy ($r = 0.37$, $P = 0.01$, FDR corrected) (Fig. 3*B*), characterized by higher activation in visual-sensory, salience, and basal ganglia networks (Fig. 2*A*). Meanwhile, another dominant state S1's occupancy shows no reliable correlation with emotional accuracy ($r = 0.19$, $P = 0.15$, FDR corrected). Among dominant states for WM task, we identified state S4 showing a negative correlation with accuracy of 2-back condition ($r = -0.25$, $P = 0.032$, FDR corrected), characterized by low activation in regions of lateral executive control network. While another dominant state S5 exhibits marginal correlation with 2-back accuracy ($r = 0.21$, $P = 0.068$, FDR corrected), characterized by activation in visual-spatial and executive control network. All correlation results under other conditions are listed in *SI Appendix*, Fig. S12.

Since brain states S8 and S4 closely linked to emotional and WM 2-back performance, we further examined CAR-related differences in fractional occupancy and mean lifetime of these two states between DXM and Placebo groups. Separate nonparametric permutation tests were implemented to account for nonnormal distribution of these brain state occupancy derived from each block during emotional and WM tasks (*Methods*). This revealed significantly higher fractional occupancy (Fig. 3*E*) and mean lifetime (*SI Appendix*, Fig. S14) of emotional state S8 in Placebo than DXM group during emotional condition ($Ps < 0.04$, FDR corrected), while no difference in state S1 ($Ps > 0.4$, FDR corrected). Parallel analysis for WM task revealed significantly higher fractional occupancy (Fig. 3*F*) and mean lifetime (*SI Appendix*, Fig. S14) of state S4 during WM 2-back condition ($Ps < 0.03$ FDR corrected) in Placebo than DXM group. However, no difference for state S5 was observed between groups ($Ps > 0.12$, FDR corrected). Results in Cohort 2 are provided in *SI Appendix*, Fig. S11.

Based on our recent observation on CAR-related lower prefrontal activity linked to better neural efficiency for WM processing (13), we speculate that our observed higher occupancy of state S4 with relatively lower activity in Placebo reflects similar phenomenon. We therefore computed an index reflecting network efficiency during WM (*SI Appendix*, Text S1), and permutation test revealed significantly higher network efficiency during 2-back in Placebo than DXM group ($P = 0.028$, FDR corrected, *SI Appendix*, Fig. S15).

To better illustrate which psychological processes are linked to brain states most dominant to rest, emotion, and WM, we employed a meta-analytic neurosynth-decoding approach to identify the most relevant terms and word cloud plots were implemented to illustrate decoding results (*Methods*). As depicted in Fig. 3*G*, brain states S2, S8, and S5 are closely associated with psychological terms that are most likely involved in rest, emotional, and WM tasks in our present study, respectively. While less reliable decoding results were identified for states S1 and S4 that are also dominant to emotional and WM tasks (*SI Appendix*, Table S1).

Together, these results indicate that suppression of CAR can lead to a decrease in factional occupancy and mean lifetime of

Downloaded from https://www.pnas.org by HEFEI UNIVERSITY OF TECHNOLOGY on December 16, 2024 from IP address 114.213.251.57.

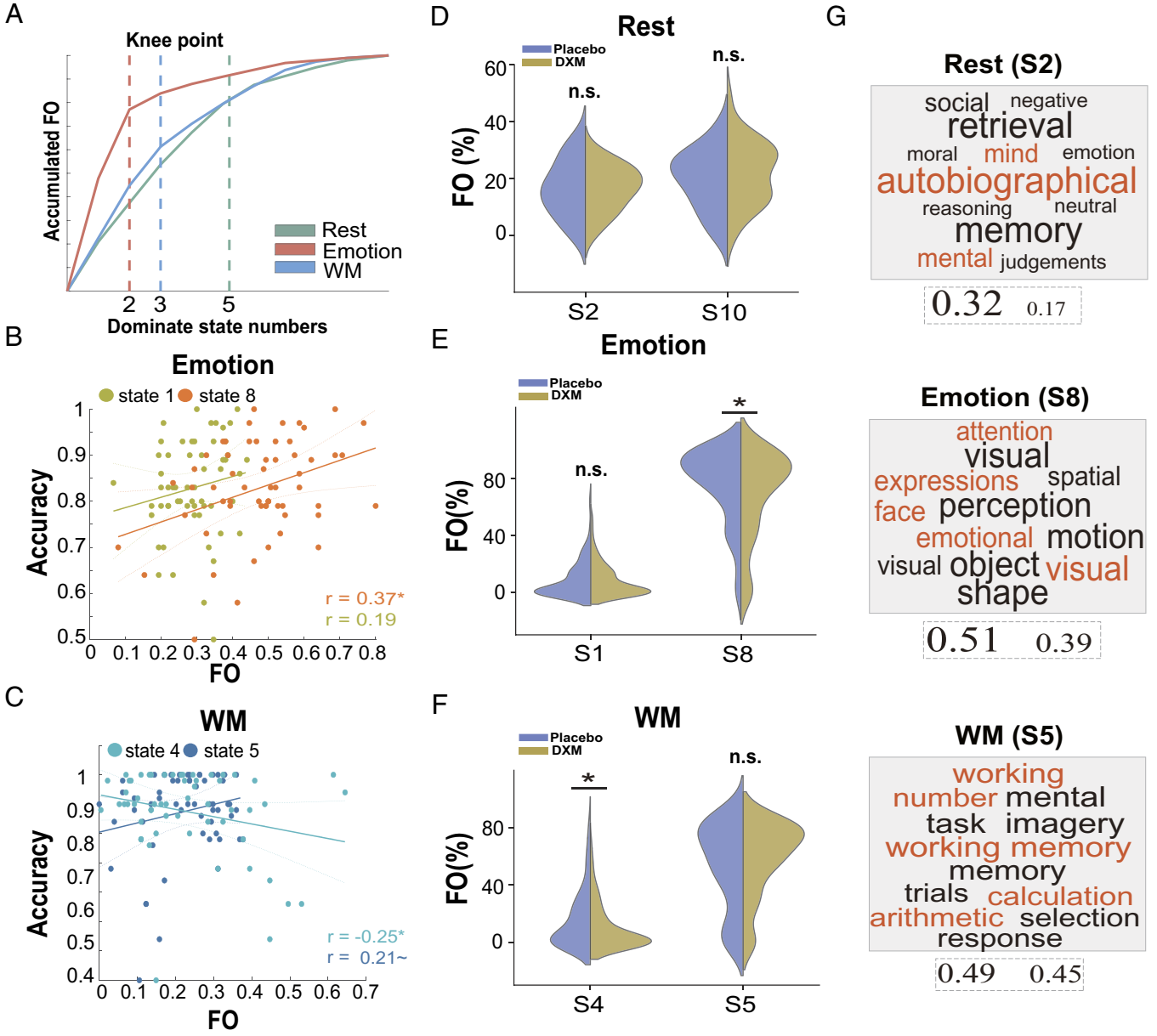

Fig. 3. Occupancy rates of dominant brain states showing significant differences between Placebo and DXM groups. (*A*) Dominant states selection based on knee point analysis and vertical dashed lines represent corresponding dominant state numbers determined by knee point for each task separately. (*B* and *C*). Correlations between fractional occupancy of dominate states in Emotion and WM task and corresponding performance. (*D–F*) Density distribution plots depict fractional occupancy of dominant states in Placebo and DXM groups under Rest, Emotion, and WM 2-back conditions. Plots are smoothed by the kernel density estimation (KDE). (*G*) Wordcloud plots for Neurosynth-based decoding terms for states of interest. The font size of each term in each plot is based on its relative decoded correlation value, and we list the top and last correlation values below each wordcloud plot with their font size relative to the correlation values. Notes: n.s., nonsignificant, ~$P < 0.10$, *$P < 0.05$, FDR corrected.

brain states (i.e., S8, S4) that are respectively dominant to Emotion and WM tasks rather than resting state. That is, the proactive effects of CAR on increased occupancy and mean lifetime of emotion- and WM-related dominant brain states.

CAR Proactive Effects on Brain State Transitions during Emotion and Executive Functions. Beyond occupancy and mean lifetime, we further investigate how CAR proactively modulates dynamic transitions among states during emotional and executive functioning to address our hypothesis on neural resource allocation. We first computed transition probability among brain states across Rest, Emotion, and WM tasks and subsequent Louvain community detection (*Methods*) identified three robust communities (Fig. 4*B* and *SI Appendix*, Fig. S16), highly consistent with the structure of dominant states based on our knee analysis. Further network-based statistics (*Methods*) revealed significantly higher transition probabilities between dominant brain states under Emotion and WM tasks, respectively (*all Ps* < 0.05, FWE corrected) (Fig. 4*C*). However, we observed no significant difference in edge-by-edge transition between Placebo and DXM groups during Rest, Emotion, or WM tasks (*all Ps* > 0.05, FWE corrected).

Beyond edge-by-edge comparisons, we further investigate whether CAR modulates system-level transition dynamics by computing sequence complexity of state transitions (namely, transition complexity) (*Methods*) during Emotion (emotion vs. neutral) and WM (2- vs. 0-back) tasks. Based on information theory (47), this approach has been implemented in deciphering the state sequence syntax of brain computations underlying sleep, anesthesia, and other task contexts, reflecting distinct modes of neural

Downloaded from https://www.pnas.org by HEFEI UNIVERSITY OF TECHNOLOGY on December 16, 2024 from IP address 114.213.251.57.

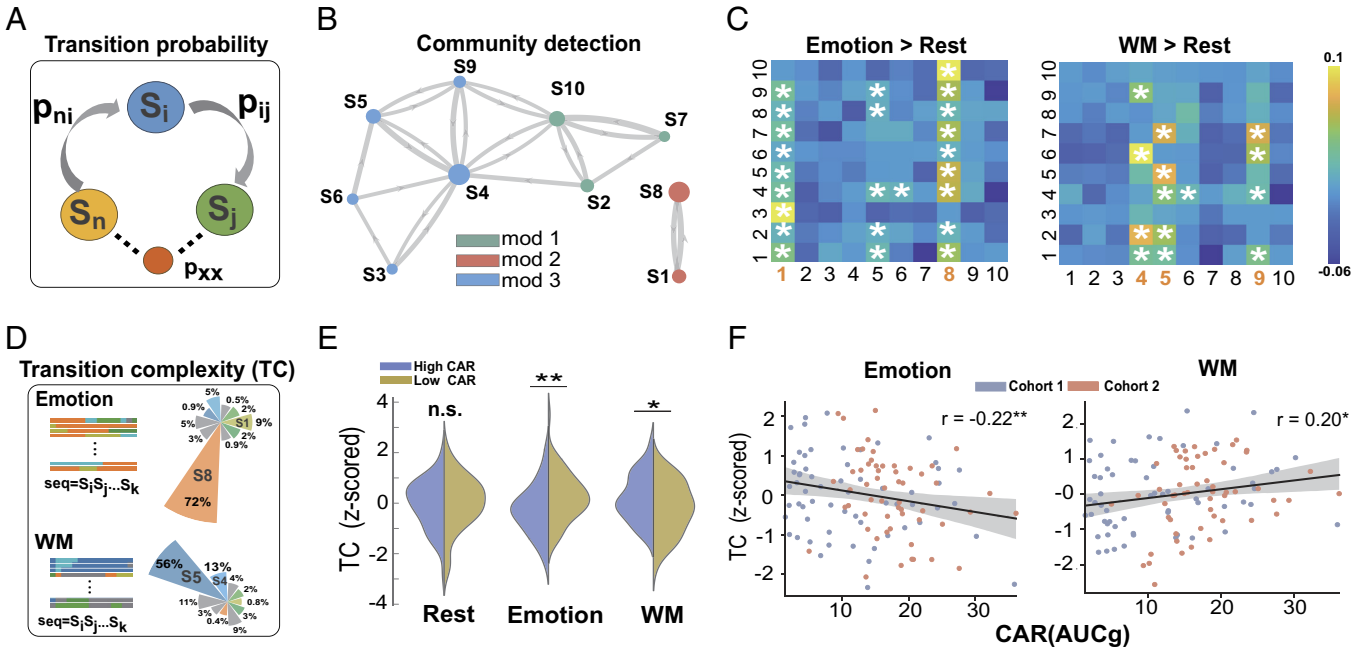

Fig. 4. State transition dynamics in Placebo and DXM groups. (*A*) An illustration for edge-by-edge transition probability between brain states. (*B*) Louvian-detected community modules (top 25% transitions) based on transition probabilities among all states across three tasks. Nodes with the same color belong to the same community. (*C*) Group-averaged transition probability difference between Emotion vs. Rest (*Left*) and WM vs. Rest (*Right*). Asterisks represent significant higher transitions of Emotion and WM compared with Rest ($P_{FWE} < 0.05$). Dominate states in Emotion and WM are highlighted. (*D*) An illustration for sequence complexity of state transition and polar area diagrams represent relative state occupancy distributions underlying emotional and 2-back WM conditions. (*E*) Density distribution plots depict transition complexity for Rest, Emotion, and WM between high and low CAR groups, by combining data from Cohorts 1 and 2. (*F*) Scatter plots depict correlations between AUCg measure of CAR and transition complexity of state sequence during Emotion (primarily anchored on visual-sensory and salience networks) and WM (anchored on executive control and visuospatial networks) processing. Notes: n.s., nonsignificance *$P < 0.05$, **$P < 0.01$, FDR corrected.

resource allocation (48). We thus implemented this transition complexity index to investigate whether CAR modulates resource allocation across emotional and WM processing. As illustrated in Fig. 4*D*, there is a clear distinction of state sequence patterns across emotion and executive functioning. Permutation tests were then conducted to test the differences when two cohorts were combined according to both AUCi and AUCg measures of CAR (*Methods*). Although we did not find reliable effects pertaining to AUCi ($Ps > 0.24$), we observed significantly higher transition complexity during emotional task ($P = 0.004$) when overall CAR (AUCg, total cortisol secretion within 1-h postawakening) was suppressed or lower according to AUCg measure. Interestingly, an opposite pattern with lower transition complexity was observed during WM processing ($P = 0.014$). Further correlation analyses revealed that individuals with lower AUCg exhibited significantly correlation with higher transition complexity during Emotion task ($r = -0.22$, $P = 0.008$). Conversely, an opposite correlation with lower transition complexity was observed during WM processing ($r = 0.20$, $P = 0.015$) when overall CAR was lower (Fig. 4*F*). Again, no reliable correlation was observed for AUCi. Notably, we also observed significant correlations when analyzing data in Cohorts 1 and 2 separately for AUCg, indicating the robustness of our observed CAR-related distinct modulations of transition complexity on emotional and WM processing (*SI Appendix*, Table S2).

Together, our above results indicate that a suppressed or lower overall CAR can lead to higher transition complexity of brain states primarily anchored onto visual-sensory and salience networks (i.e., S8) during Emotion task, but an opposite pattern of lower transition complexity of brain states anchored onto executive control and visuospatial networks (i.e., S5, S4) during WM task. These results exhibit differential modulation patterns of CAR on system-level transition complexity during Emotion and WM processing, suggesting a proactive role of CAR in modulating allocation of neural resources across emotional and executive functions.

Discussion

By leveraging pharmacological neuroimaging and HMM, we investigate how CAR proactively modulates dynamic reconfiguration of brain networks across emotional and executive functions. As expected, suppression of CAR in the morning proactively impaired emotional discrimination for negative facial expressions but not WM performance, while individuals with lower CAR exhibited poorer performance of both emotional and WM (2-back) tasks later in the afternoon of the same day. In parallel, suppression of CAR led to a general decrease in fractional occupancy and mean lifetime of two task-specific brain states dominant to emotional and WM processing. Further information-theoretic analysis revealed that a suppressed/lower overall CAR led to higher transition complexity of brain states (primarily anchored on visual-sensory and salience as well as basal ganglia networks) during emotion task, but an opposite pattern of transition complexity for brain states (anchored on visuospatial and executive control networks) toward WM, suggesting CAR-mediated distinct proactive modulations on optimizing a flexible allocation of neural resources across emotional and executive functions. Collectively, our findings establish a causal link of CAR in the morning and its proactive modulation on emotional and executive functions. As we will discuss below, these findings are most likely resulted from interplay of CAR-mediated tonic activity and task-induced rapid reconfiguration of large-scale functional brain networks to enable flexible allocation of neurocognitive resource, under a framework of human allostasis.

Downloaded from https://www.pnas.org by HEFEI UNIVERSITY OF TECHNOLOGY on December 16, 2024 from IP address 114.213.251.57.

CAR Facilitates Emotional and Executive Functions Via Optimizing Dynamic Organization of Task-Specific Dominant Brain States. As expected by our first hypothesis, we observed the proactive effects of CAR on emotional and WM performance: suppression of CAR selectively impaired accuracy for discriminating negative facial expressions in DXM (vs. Placebo) group, while individuals with lower CAR exhibited poorer accuracy for both emotional and WM 2-back tasks. These effects are in line with behavioral improvement in normative CAR and impairment in lower/blunted CAR in literature (9, 13, 49). Although no group difference emerged, our observed positive correlation of CAR (AUCi) with WM 2-back accuracy is consistent with our recent observations (13), suggesting improved neural efficiency during WM discussed in next section. Based on psychological and neurobiological views of CAR (7–9), we speculate that our observed CAR proactive effects on emotional and WM performance could be resulted from CAR-induced tonic modulations that come to play even several hours after its first burst in the morning, most likely via the relatively slow genomic actions (3, 27, 28) and interplay with task-dependent neurotransmitters (28) as discussed below.

On the neuroimaging level, suppression of CAR led to lower occupancy and mean lifetime of two task-induced brain states (i.e., S8, S4) that are dominant to emotional and WM processing, respectively. This finding is innovative, as our study targets on CAR effects on brain network dynamics, extending previous studies focusing on local regions (13, 39, 50, 51). The observed CAR proactive effects on task-specific brain states support our hypothesis that interplay between CAR in the morning and task-dependent neurotransmitters indeed jointly modulates brain network dynamic reconfigurations across emotional and executive functions, suggesting that neuroendocrinal crosstalk is essential to enable cognitive flexibility and adaptation for ever-changing challenges. Specifically, brain state (S8) dominant to emotional processing is characterized by higher engagement of visual-sensory, salience, and basal ganglia networks (including thalamus and caudate). Notably, the thalamus and caudate of the striatum can be also classified into the salience network in a broader definition (39, 52). Thus, our observed activity pattern of S8 could be associated with attentional vigilance to salient stimuli during emotional task. Indeed, our Neurosynth-decoded results confirm this state linked to mental processes of emotional expression and face recognition. Based on previous studies (53, 54), emotional stimuli-induced phasic activity of noradrenaline from locus coeruleus (LC) targeting to limbic structures and basal ganglia could substantially modulate neuronal excitability. Activation of these regions along with high-level visual–sensory network can reflect the engagement of goal-directed visual attention for emotional stimuli (39, 55, 56). Thus, through GR-mediated tonic actions CAR's interaction with task-dependent phasic noradrenaline activity could promote coactivation of these networks vital for attention and emotional salience processing, in line with our observed CAR-induced proactive increase in emotional brain state occupancy and improvement in corresponding performance, further supporting our hypothesis.

Moreover, suppression of CAR is correlated with lower occupancy and mean lifetime of brain state S4 during WM 2-back task, characterized by lower activity of lateral executive network regions. In other words, normative CAR can lead to higher occupancy and mean lifetime of this brain state. Based on insights from previous studies (13, 57), weaker activity in regions of this network may reflect greater neural efficiency, likely by utilizing less resources to achieve comparable WM performance (57, 58). This notion is supported by two pieces of our results: 1) higher occupancy of state S4 with low engagement in regions of executive control network in Placebo than DXM group, 2) higher network efficiency of this state during 2-back task in Placebo than DXM group. These findings are also in line with predictions by the influential neurobiological models suggesting that GR-mediated genomic actions can interact with task-driven D1-receptor mediated phasic dopaminergic activity to support WM processing (28), possibly leading to increased efficiency to support executive functioning (59). Together, our above findings point toward that CAR proactively facilitates emotional and executive functions, most likely through an interplay between CAR-mediated tonic activity and task-invoked catecholaminergic actions that increase excitability and activity of emotion- and WM-related brain networks.

CAR Proactively Modulates Dynamic Neural Resource Allocation Across Emotional and Executive Functions. Beyond above effects on task-specific state occupancy and mean lifetime, our second hypothesis addresses CAR's proactive effects on neural resource allocation across emotional and executive functions. By quantifying sequence complexity of state transitions, we observed significantly higher transition complexity during emotion task while opposite pattern with lower transition complexity during WM task, when CAR was suppressed or lower as measured by overall CAR (i.e., AUCg within 1-h post awakening). Such transition complexity is thought to represent a syntax-based mode of information processing (43), and changes in transition complexity of one system may reflect an alteration of resource allocation. Thus, our observed opposite patterns of transition complexity may reflect flexible resource allocation toward emotion and WM processing that anchors onto distinct functional brain network configurations. Specifically, our observed higher transition complexity during emotion processing when CAR was suppressed or lower in the normative CAR condition may reflect a flexible resource allocation to enable rapid reconfiguration of visual-sensory and salience networks (i.e., dominant state S8) for quick detection and processing emotionally laden stimuli, similar to the consequence when facing acute stress (33). Conversely, an opposite pattern of transition complexity under high-load WM may reflect a more deliberate mode of resource allocation toward functional organization of the executive control and visuospatial networks (i.e., dominant states such as S5 and S4) for optimizing WM processing, which requires flexibly updating and maintaining the most recent two items in mind to perform 2-back task under executive control. Notably, such distinct modulations of resource allocation are further supported by our observed opposite correlations between overall CAR (AUCg) and transition complexity during emotional and WM tasks.

According to neuroendocrinal and neuromodulatory studies, both stress-induced slow corticosteroid effect (39, 60) and stimuli-induced phasic norepinephrine actions (29, 38, 40) can indeed regulate neuronal excitability/gain and up-regulate mesoscopic neural networks across distinct neurocognitive domains, as indicated by recent computational studies (37, 41). We believe interactions between CAR-initiated tonic activity and task-dependent phasic catecholaminergic actions could leverage similar integrative strategy of modulating resource allocation across distinct neurocognitive domains to support optimal adaptability and flexibility for ever-changing demands, further fostering allostasis of the neurobiological systems (1, 2, 61). Thus, our observed alterations in transition complexity during emotional and WM processing may have important implications in CAR-mediated proactive effects, through actively modulating neural resource allocation for cognitive and behavioral flexibility, thereby serving as a crucial role in supporting system allostasis (1, 36). Together, our findings provide evidence that CAR proactively modulates neural resource allocation across emotional and executive functioning.

Downloaded from https://www.pnas.org by HEFEI UNIVERSITY OF TECHNOLOGY on December 16, 2024 from IP address 114.213.251.57.

It is worth to note that an overall AUCg rather than AUCi measure of CAR could reliably account for system-level state transitions reflecting dynamic resource allocation. This may originate from an integrative nature of AUCg measure that constitutes both basal (trait-like) and dynamic (state-like) components of CAR after postawakening in relation to the overall HPA-axis activity, according to theoretical implications of these two distinct measures in the neuroendocrinology and psychology (7, 62, 63). Future studies should disentangle their distinct roles in modulating brain network dynamics and their links to allostasis.

Our study has several limitations. First, our study focused on CAR in males attempting to avoid confounds by female menstrual cycles, which may impede the generalizability into female populations. Second, our study did not include concurrent measures of physiological activity and task-induced transient modulators that may interplay with CAR. Third, our study did not collect fMRI data in morning, and future studies with optimal designs are crucial to address the mechanisms underlying time-dependent effects of CAR spanning over morning and afternoon. Innovative neuroimaging techniques with much denser sampling sessions are also required to examine how interplay of CAR with task-induced phasic neuromodulators affects human emotion and cognition throughout the day.

In conclusion, our study demonstrates the proactive effects of CAR on dynamic reconfiguration of large-scale brain networks across emotional and executive functions. Our findings establish a causal link of how CAR proactively modulates brain network dynamics via acting on task-specific brain state occupancy and system-level transition dynamicity of brain network reconfigurations, suggesting a neuroendocrinal model underlying flexible allocation of neural resources across emotional and cognitive demands. Our findings provide insights into CAR-mediated proactive effects that may serve as a key role in human allostasis to enable brain preparedness for upcoming challenges.

Methods

Participants. A total of 122 young, healthy, male college students were recruited in two cohorts, with 62 participants (mean age: 22.9 ± 1.9; range: 18 to 27 y old) in Cohort 1 and 60 participants in Cohort 2 (mean age: 21.6 ± 0.8; range: 20 to 24 y old). Given hormonal fluctuations during the periodic menstrual cycle in females may impede a reliable assessment of the normative CAR, female participants were not included in the present study. All participants reported no history of neurological, psychiatric, or endocrinal disorders. We first excluded participants if these factors did not meet the requirements: tobacco or alcohol use, irregular sleep/wake rhythm, intense daily physical exercise, abnormal hearing or vision, predominant left-handedness, current periodontitis, stressful experience, or major life events. More details can be found in our previous study (13). Informed written consent was obtained from each participant before the experiment and study protocol was approved by the Institutional Review Board for Human Participants at Beijing Normal University. The protocol with pharmacological manipulation was registered as a clinical trial before the experiment (https://register.clinicaltrials.gov/; Protocol ID: ICBIR_A_0098_002). We excluded participant if their mean frame-wise displacement is over 0.2 mm or motion spike over 5 mm during fMRI scanning (64, 65). Based on this criterion, two participants were excluded from further analyses and one participant's spikes was over 5 mm only during rest and we kept data of this participant for Emotion and WM analyses.

Pharmacological Manipulations. For Cohort 1, participants were randomly assigned into the CAR-suppressed or control group. We employed the randomized, double-blind pharmacological manipulations on Day 1 night and we mainly focused on CAR assessment on Day 2 to address our hypotheses on the proactive effects of the CAR on brain state dynamics during rest, emotional, and WM processing. Participants in the experimental group received a dose of 0.5 mg Dexamethasone (namely DXM group) and the control group received equal amount of Vitamin C (placebo group) at 20:00 on Day 1. Based on our pilot experiment, the choice of the time at 20:00 was to ensure that the suppressed CAR in the DXM group would restore to a normal and overlapped level with placebo group when conducting fMRI scanning in the afternoon (*SI Appendix*, Fig. S1). This design allows us to test the CAR proactive effects aligning with our central hypothesis, by mitigating potential confounds of elevated cortisol levels during fMRI scanning in afternoon. In Cohort 1, to capture the diurnal cortisol responses as a function of time from morning to evening, we used a time-stamped dense sampling approach to collect a total of 15 saliva samples over three consecutive days (Fig. 1): Day 1 at 22:00, Day 2 at 7:00 (awakening time), 7:15 (15 min after awakening), 7:30 (30 min after awakening), 8:00 (1 h min after awakening), 11:00 before lunch, before and after fMRI scanning in the afternoon from 14:00 to 17:00 and 22:00 in the evening; Day 3 at 7:00 (awakening time), 7:15 (15 min after awakening), 7:30 (30 min after awakening), 8:00 (1 h min after awakening), and the final 2 sampling at 11:00 and 16:00, respectively. Saliva samples were collected using Salivette collection device (Sarstedt, Germany). Notably, participants' subjective mood ratings were assessed across 3 via Positive and Negative Affect Schedule (PANAS) and no group differences were observed in both positive and negative scores across 3, further ruling out potential influences by subjective mood (*SI Appendix*, Fig. S3).

An independent Cohort 2 with natural assessment of the CAR and similar task designs was included to serve as a complementary purpose to further examine the robustness of major results from pharmacological cohort. In Cohort 2, we collected morning cortisol samples within 1 h immediately postwakening from two consecutive days. A total of 10 saliva samples were collected at 0, 15, 30, and 60 min after awakening on both Day 2 and Day 3. Extra 2 time points before and after fMRI scanning on Day 2. Notably, three participants in Cohort 2 who had missing saliva samples among the first four collected on Day 2 were excluded from further CAR-related analyses.

We took several stringent procedures to assure that saliva samples were not affected by other factors of no interest, including: 1) participants were asked not to brush teeth, drink, or eat within 1 h before sampling, 2) participants were required to refrain from any alcohol, coffee, nicotine consumption, and excessive exercise at least 1 before experiment. Saliva samples were returned back to the laboratory and kept frozen (−20 °C) until assay. After thawing and centrifuging at 3,000 rpm for 5 min, the saliva samples were analyzed using an electrochemiluminescence immunoassay (ECLIA, Cobas e601, Roche Diagnostics, Mannheim, Germany) with sensitivity of 0.500 nmol/L. Intra- and interassay variations were below 10%.

Two measures of CAR were computed by using AUCi and AUCg in our present study. Specifically, AUCi is denoted as the Area Under the Curve with respect to increase by the equation: AUCi = (S1 + S2) × 15 min/2 + (S2 + S3) × 15 min/2 + (S3 + S4) × 30 min/2 − S1 × (15 min +15 min + 30 min), while AUCg is denoted as the Area Under the Curve with respect to ground, which is equal to AUCi plus a basal-cortisol activity within 1 h after awakening: AUCg = (S1 + S2) × 15 min/2 + (S2 + S3) × 15 min/2 + (S3 + S4) × 30 min/2. Based on the guideline consensus of the field, AUCi and AUCg may yield dissociable yet related psychoendocrinal meanings of postawakening secretion of cortisol: AUCi is believed to reflect a diurnal/dynamic (state-like) change of CAR over time, while AUCg may reflect the overall (trait-like) cortisol secretion of postawakening including AUCi (9, 66). Note that part of the endocrinal data along with WM task were also used in our previous study (13).

Emotional and Cognitive Tasks. At Day 2 afternoon, participants went through consecutive multiple tasks involving Resting state, emotion discrimination (Emotion), and N-back WM tasks. During rest, participants were instructed to open the eyes, relax, and be still and scanning duration for 348 s. During emotion task, participants performed a discrimination of negatively emotional facial expressions versus sensorimotor control task. The task consisted of 10 blocks, each block containing six trials of images. Each block started with a cue for 5 s indicating either emotion or control condition, after which six trials of images were presented 5 s each. For emotion block, participants need to select the emotional face from two candidate faces in the bottom of the screen that expressed the same emotion as the target expression on the top of the screen. For control condition, participants viewed the same number of trials of images and each block started with a cue for 5 s. Thereafter, participants need to select the scrambled shapes from two candidate shapes in the bottom of the screen that expressed the same shape as the target shape on the top of the screen. Notably, only negative facial expressions were included in the present study.

Downloaded from https://www.pnas.org by HEFEI UNIVERSITY OF TECHNOLOGY on December 16, 2024 from IP address 114.213.251.57.

For the N-back WM task, it consisted of 12 blocks of alternating 0-, 1-, and 2-back conditions. Each block started with a 2-s cue indicating the experimental condition, followed by a pseudorandomized sequence consisting of 15 digits. Each digit was presented for 400 ms followed by an interstimulus interval of 1,400 ms. Blocks were interleaved by a jittered fixation ranging from 8 to 12 s, resulting in a mean interblock duration of 38 s. During 0-back condition, participants need to detect whether the current digit was "1." During the 1-back condition, participants were instructed to detect whether the current digit is the same with digit appeared 1 position back in the sequence. During the 2-back condition, participants were instructed to detect whether the current digit is the same with digit appeared 2 positions back in the sequence. Each sequence contained either 2 or 3 targets and participants were asked to make a button press with their right index finger as fast as possible when detecting a target. The employment of 3 distinct tasks for participants is to elicit sufficient and distinct cognitions covering most brain networks and better capture the dynamic shifts induced by CAR. This multitask procedure is proven to be efficient in eliciting distinct whole-brain network configurations in other studies focusing on network dynamicity (67, 68).

For Cohort 2, the task procedure and design are the same with Cohort 1, with consecutive tasks of rest, emotion, and WM tasks. During WM, we adopted a simplified design with only two WM loads (i.e., 0- and 2-back) and six blocks of each condition. Emotion task contains total 10 blocks, with an unequal number of emotional and neutral condition blocks. We thus selected the first four blocks from emotion and neutral condition respectively for subsequent analyses. Other parameters are the same with Cohort 1.

Behavioral Data Analysis. Separate ANOVAs were conducted for accuracy of emotional and WM tasks. We excluded participants with poor accuracy if their accuracy in each task condition is below the mean by three from further behavioral data analyses. This criterion led to two participants for emotion task and 5 ones for WM task excluded in Cohort 1. Further behavior-brain association analyses in specific condition (0\1\2-back and emotion\neutral) were conducted by excluding relevant data with poor accuracy in that condition.

Brain Imaging Data Acquisition. Whole-brain images in both Cohorts were acquired on a Siemens 3.0 T TRIO MRI scanner (Erlangen, Germany) in the National Key Laboratory of Cognitive Neuroscience and Learning & IDG/McGovern Institute for Brain Research at Beijing Normal University. Functional brain images were consecutively collected during resting state, emotion matching, and N-back WM tasks, using gradient-recalled echo planar imaging (GR-EPI) sequence (axial slices = 33, volume repetition time = 2.0 s, echo time = 30 ms, flip angle = 90, slice thickness = 4 mm, gap= 0.6 mm, field of view = 200 × 200 mm, and voxel size = 3.1 × 3.1 × 4.6 mm). T1-weighted 3D magnetization-prepared rapid gradient echo sequence (slices = 192, volume repetition time = 2,530 ms, echo time = 3.45 ms, flip angle = 7°, slice thickness = 1 mm, field of view = 256 × 256 mm, voxel size = 1 × 1 × 1 mm^3).

Functional Data Preprocessing and BOLD Time Series Extraction. Image preprocessing was performed using Statistical Parametric Mapping (SPM12, http://www.fil.ion.ucl.ac.uk/spm). Preprocessing steps include 1) removing the first four volumes of functional images for rest, emotion, and WM tasks respectively, for signal equilibrium, 2) correcting for slice-timing acquisition, 3) realigned for head motion correction, 4) coregistered to the gray matter image segmented from subject's own anatomical T1-weighted images, 5) spatially normalized into common stereotactic MNI space, and 6) images were finally resampled into 2-mm isotropic voxels and smoothed by isotropic 3-D Gaussian kernel with 6 mm full-width at half-maximum. We employed a predefined 14 networks template, covering wide-spread cognitive and affective processing regions that have been widely studied (44, 69–71). We next extracted preprocessed BOLD time series for each task by using the 14 network templates, which results in a time series matrix (14 brain networks) × (task durations). For Cohort 1, time series matrix for rest is 14-by-170, for emotion task is 14-by-150 and for N-back WM task is 14-by-228. For Cohort 2, time series matrix for rest is 14 × 176, for emotional task is 14-by-150 and for N-back is 14-by-228. For both Cohorts, time series were high-pass filtered at 0.008 Hz after which the white matter and cerebrospinal fluid, as well as 24-head movement signals were further used as regressor to remove out from time series. Then, preprocessed time series of 14 networks for the three tasks were temporally concatenated together for each participant, yielding a 14-by-548 time series matrix for Cohort 1 and 14-by-554 time series matrix for Cohort 2. The concatenated time series were normalized per column to yield 0 mean and 1. Finally, normalized time series matrices for each participant were combined to yield a N-by-14-by-T participants matrix ready for the HMM where N and T represent the number of participants and the length of time series for three tasks.

HMM for Multiple Tasks. We implemented HMM toolbox (https://github.com/OHBA-analysis/HMM-MAR) to estimate spatiotemporal configurations of functional brain networks, as it enables us to quantify time-resolved brain state dynamics (Vidaurre et al., (72)). The HMM considers a set of multidimensional input signals that can be modeled as a sequence of latent discrete states occurring and omitting as time evolves. Each state is defined as both mean of each dimension and covariance among each dimension, generated by the Gaussian distribution. Through Bayesian variations as well as Markovian process, HMM could infer discrete brain states that represent a repertoire of a number of canonical brain networks via Viterbi decoding (Vidaurre et al., (72)). Moreover, the unique feature of this method is that it could compute fractional occupancy, mean lifetime as well as transition dynamics. These dynamic features could help elucidate the rapid reorganization of brain networks among various cognitive and affective processing. Here, we consider that the human brain dynamically reconfigures distinct brain networks to meet ever-changing requirement of external cognitive and affective tasks. As such, we employed a set of 14 canonical brain networks derived by Shirer et al. (73) as predefined ROIs to cover potential network interactions during multiple tasks. These ROIs have been widely used by previous studies focusing on large-scale functional brain networks (44, 74). After extracting time series from three tasks, we concatenated them and conducted HMM. Akin to previous studies (44–46), free energy as well as Akaike Information Criterion (AIC) was computed at a range from 2 to 16 states with a step of 2 (*SI Appendix*, Fig. S6). We found that 10 states are sufficiently to capture brain sate dynamics across Rest, Emotion, and WM tasks, and expanding state numbers yields redundant states which are rarely occupied and the relative percentage change in free energy and AIC becomes negligible. The HMM model yielded several major output metrics: 1) State assignment for each time point, each subject, via Viterbi path decoding, based on which we calculated individual-level fractional occupancy (FO) and mean lifetime for each state under each specific task (Rest\Emotion\WM) or block-based condition (0\1\2-back and emotion\neutral) and compared group differences. 2) Each state's estimated relative magnitude across 14 brain networks (Fig. 2*A*), representing relative engagement of each network under each certain brain state. 3) Individual-level transition matrices among 10 distinct states under each task were computed by the likelihood of switching between pair of specified states according to any given task.

t-SNE Embedding Visualization. To capture the distribution structure under Rest, Emotion, and WM tasks, we utilized a t-distributed stochastic neighbor embedding (t-SNE) visualization technique (75), which can represent high-dimensional data into a reduced dimension while preserving the local distances between data points. In our study, we defined states distribution under task condition as a 10-element vector, each element in the vector represents relative fractional occupancy of brain states per task. As such, we created the distribution vectors for all 3 tasks for each subject, and we then employed t-SNE analysis to plot the low-dimensional distribution clusters across each task per participant and visualize the relative distance among them.

Knee Point Analysis. A knee point analysis based on previous study (76) was employed to determine the dominant states for each condition. We first ranked average fractional occupancy of all brain states under rest, emotion matching, and n-back tasks, separately. Then, we calculated accumulative fractional occupancy curve and employed "kneedle" algorithm (77) to detect knee point, defined by a significant transient point in the maximum curvature, as a threshold to select the most dominant states for each task (*SI Appendix*, Fig. S10). After that, we conducted multiple comparisons correction based on these dominant states detected by knee point analysis for subsequent statistical analyses under each task.

Neurosynth-Based Decoding analysis. To reveal the potential neurocognitive processes associated with each state feature, we took advantage of meta-analysis using reverse-inferred similarity-based algorithm by the CANlab toolbox (https://canlab.github.io/). Consistent with previous studies (44, 78), we correlated each state's activation pattern with the topic term-derived maps from the large-scale

Downloaded from https://www.pnas.org by HEFEI UNIVERSITY OF TECHNOLOGY on December 16, 2024 from IP address 114.213.251.57.

Neurosynth platform including 11,406 studies. For each state of interest, we chose the first 4 topics with highest correlations, under which we further chose the first three terms of each topic. This ends up a total of 12 terms for each state ready for Wordcloud visualization. Notably, we manually excluded terms representing irrelevant processes, and merged the similar terms (e.g., face\facial) until the included terms reached 12. Finally, we implemented each state's related terms in a Wordcloud plot and the size of each term is based on its relative correlation value.

Community Detection and Network-Based Statistics for State Transition Probability. To detect potential transition modules among states under each task, we obtained transition matrix across rest, emotional, and WM tasks derived from HMM model. Then, we employed Louvian community detection algorithm to estimate clustering modules in the network of transition matrix. We set different thresholds for the inclusion of transitions (top 15%, 20%, 25%, and 40%, respectively) before conducting community detection to test the robustness of clustering results (*SI Appendix*, Fig. S16). To further investigate task and group differences in state transition dynamics, we implemented network-based statistics (v1.2) (79) to compare: i) transition differences between emotion task versus rest as well as WM task versus rest, respectively; ii) group differences in transition matrices between Placebo and DXM under rest, emotion, and WM tasks, separately. Significance determination was computed via nonparametric permutations setting at 5,000, alpha setting at 0.05, FWE correction.

Transition Complexity of State Sequence. To assess the system-level transition dynamics as an indicator of neurocognitive resource allocation, we implemented transition complexity index adapted from information-theoretic methods in previous studies (47, 48). This algorithm is derived from information theory and defines a given sequence as symbolic streams of words and measures the complexity of a given state sequences based on to what extent the list can be compressed into a shorter version of sequence without losing information of that sequence. Based on information theory (47), this approach has been implemented in deciphering the state sequence syntax of neural computations underlying sleep, anesthesia, and other task contexts, reflecting distinct modes of neural resource allocation (48). We implemented this transition complexity index to investigate whether CAR modulates resource allocation across emotional and WM processing. According to the neurobiological models of CAR and our hypothesis, we speculate that alteration of such transition complexity could be linked to dynamic resource allocations. We then conducted group comparisons and correlation analyses for transition complexity metrics in Emotion (emotion vs. neutral) and WM (2- vs. 0-back) via combining Cohort 1 and 2. For group comparison of transition complexity, we split participants from Cohort 2 into higher\lower AUCg as well as higher\lower AUCi measures of CAR, based on the criterion in previous studies (5, 63) and then combined with Placebo\DXM groups in Cohort 1 accordingly. For correlational analyses between CAR and transition complexity, we z-scored transition complexity metrics in each cohort separately before combining data from two Cohorts.

Permutation Testing. To better account for the distributions of behavioral (i.e., accuracy) and brain state measures (i.e., fractional occupancy, mean lifetime, and transitions) that may not meet the normality assumption, we conducted nonparametric permutation tests to perform the statistical inference and determine the significance. For group comparisons of brain state measures, we randomly shuffled group labels between Placebo and DXM groups and calculated the difference in mean values between the shuffled groups (5000 times). This process generated an empirical null distribution, and the *P*-value was determined by dividing the number of times the actual group difference exceeded the differences in the null distribution. The same procedures were conducted for group comparisons of transition complexity. For correlations between brain state occupancy and behavioral performance, we randomly shuffled the labels between each state's fractional occupancy and behavioral performance and then computed correlation value (5000 times) to generate the null distribution. We determined the *P*-value by dividing the number of times for the actual correlations exceeded the null distribution of correlations. The same procedure was also conducted for correlation analyses between CAR measures and behavioral performance as well as between CAR measures and transition complexity metrics.

Data, Materials, and Software Availability. Preprocessed BOLD-fMRI time series, endocrinal, physiological, behavioral data and trained models used for generating results in the present study are available at GitHub repository (80). The original neuroimaging data that support this study are available from the corresponding author upon reasonable request.

ACKNOWLEDGMENTS. This study has been supported by the Scientific and Technological Innovation 2030-Major Projects 2021ZD0200500, the National Natural Science Foundation of China (32130045, 32361163611, and 82021004), the Major Project of National Social Science Foundation (19ZDA363 and 20&ZD153), and the Fundamental Research Funds for the Central Universities (2024-JYB-XJSJJ020, 310422131, and 310400209508)

Author affiliations: [a]School of Management, Beijing University of Chinese Medicine, Beijing 100029, China; [b]State Key Laboratory of Cognitive Neuroscience and Learning & International Data Group/McGovern Institute for Brain Research, Beijing Normal University, Beijing 100875, China; [c]Beijing Key Laboratory of Brain Imaging and Connectomics, Beijing Normal University, Beijing 100875, China; [d]Beijing Key Laboratory of Applied Experimental Psychology, National Demonstration Center for Experimental Psychology Education (Beijing Normal University), Faculty of Psychology, Beijing Normal University, Beijing 100875, China; [e]School of Education Sciences, Chongqing Normal University, Chongqing 401331, China; [f]School of Psychology, Shenzhen University, Shenzhen 518060, China; and [g]Chinese Institute for Brain Research, Beijing 100069, China

Author contributions: Y.Z., B.X., and S.Q. designed research; Y.Z., B.X., C.L., C.C., J.W., and S.Q. performed research; Y.Z., B.X., H.G., and S.Q. analyzed data; and Y.Z., J.W., and S.Q. wrote the paper.

1. B. S. McEwen, H. Akil, Revisiting the stress concept: Implications for affective disorders. *J. Neurosci.* **40**, 12–21 (2020).
2. N. Bobba-Alves, R.-P. Juster, M. Picard, The energetic cost of allostasis and allostatic load. *Psychoneuroendocrinology* **146**, 105951 (2022).
3. E. R. de Kloet, M. Joëls, F. Holsboer, Stress and the brain: From adaptation to disease. *Nat. Revi. Neurosci.* **6**, 463–475 (2005).
4. S. J. Lupien, B. S. McEwen, M. R. Gunnar, C. Heim, Effects of stress throughout the lifespan on the brain, behaviour and cognition. *Nat. Rev. Neurosci.* **10**, 434–445 (2009).
5. A. Clow, L. Thorn, P. Evans, F. Hucklebridge, The awakening cortisol response: Methodological issues and significance. *Stress* **7**, 29–37 (2004).
6. I. Wilhelm, J. Born, B. M. Kudielka, W. Schlotz, S. Wüst, Is the cortisol awakening rise a response to awakening? *Psychoneuroendocrinology* **32**, 358–366 (2007).
7. R. Law, A. Clow, "Chapter 8: Stress, the cortisol awakening response and cognitive function" in *International Review of Neurobiology*, A. Clow, N. Smyth, Eds. (Academic Press, 2020), **vol. 150**, pp. 187–217.
8. E. Fries, L. Dettenborn, C. Kirschbaum, The cortisol awakening response (CAR): Facts and future directions. *Int. J. Psychophysiol.* **72**, 67–73 (2009).
9. A. Clow, F. Hucklebridge, T. Stalder, P. Evans, L. Thorn, The cortisol awakening response: More than a measure of HPA axis function. *Neurosci. Biobehav. Rev.* **35**, 97–103 (2010).
10. R. Sapolsky, A. Bartolomucci, Making sense of the costs of adversity throughout the lifespan on aging in humans and other animals. *Neurosci. Biobehav. Rev.* **159**, 105571 (2024).
11. A. S. Moriarty *et al.*, Cortisol awakening response and spatial working memory in man: A U-shaped relationship. *Hum. Psychopharmacol. Clin. Exp.* **29**, 295–298 (2014).
12. T. Tian *et al.*, Socioeconomic disparities affect children's amygdala-prefrontal circuitry via stress hormone response. *Biol. Psychiatry* **90**, 173–181 (2021), 10.1016/j.biopsych.2021.02.002.
13. B. Xiong *et al.*, Brain preparedness: The proactive role of the cortisol awakening response in hippocampal–prefrontal functional interactions. *Prog. Neurobiol.* **205**, 102127 (2021).
14. P. Sterling, Allostasis: A model of predictive regulation. *Physiol. Behav.* **106**, 5–15 (2012).
15. T. W. Buchanan, S. Kern, J. S. Allen, D. Tranel, C. Kirschbaum, Circadian regulation of cortisol after hippocampal damage in humans. *Biol. Psychiatry* **56**, 651–656 (2004).
16. E. R. de Kloet, S. F. de Kloet, C. S. de Kloet, A. D. de Kloet, Top-down and bottom-up control of stress-coping. *J. Neuroendocrinol.* **31**, e12675 (2019).
17. J. Herbert *et al.*, Do corticosteroids damage the brain? *J. Neuroendocrinol.* **18**, 393–411 (2006).
18. S. Cornelisse, M. Joëls, T. Smeets, A randomized trial on mineralocorticoid receptor blockade in men: Effects on stress responses, selective attention, and memory. *Neuropsychopharmacology* **36**, 2720–2728 (2011).
19. M. Joëls, E. R. de Kloet, Control of neuronal excitability by corticosteroid hormones. *Trends Neurosci.* **15**, 25–30 (1992).
20. S. Qin, E. J. Hermans, H. J. F. van Marle, J. Luo, G. Fernández, "Acute psychological stress reduces working memory-related activity in the dorsolateral prefrontal cortex." *Biol. Psychiatry* **66**, 25–32 (2009).
21. D. S. Bassett *et al.*, Dynamic reconfiguration of human brain networks during learning. *Proc. Natl. Acad. Sci. U.S.A.* **108**, 7641–7646 (2011).
22. S. L. Bressler, V. Menon, Large-scale brain networks in cognition: Emerging methods and principles. *Trends Cogn. Sci.* **14**, 277–290 (2010).
23. D. Vidaurre *et al.*, Discovering dynamic brain networks from big data in rest and task. *NeuroImage* **180**, 646–656 (2018).
24. L. Zhuang *et al.*, Rapid neural reorganization during retrieval practice predicts subsequent long-term retention and false memory. *Nat. Hum. Behav.* **6**, 134–145 (2022).
25. B. Roozendaal, B. S. McEwen, S. Chattarji, Stress, memory and the amygdala. *Nat. Rev. Neurosci.* **10**, 423–433 (2009).
26. A. H. Van Stegeren, O. T. Wolf, W. Everaerd, S. A. Rombouts, Interaction of endogenous cortisol and noradrenaline in the human amygdala. *Prog. Brain Res.* **167**, 263–268 (2007).

Downloaded from https://www.pnas.org by HEFEI UNIVERSITY OF TECHNOLOGY on December 16, 2024 from IP address 114.213.251.57.

27. M. Joëls, T. Z. Baram, The neuro-symphony of stress. *Nat. Rev. Neurosci.* **10**, 459–466 (2009).
28. A. F. T. Arnsten, Stress signalling pathways that impair prefrontal cortex structure and function. *Nat. Rev. Neurosci.* **10**, 410–422 (2009).
29. G. Aston-Jones, J. D. Cohen, An integrative theory of locus coeruleus-norepinephrine function: Adaptive gain and optimal performance. *Annu. Rev. Neurosci.* **28**, 403–450 (2005).
30. J. E. LeDoux, Emotion circuits in the brain. *Annu. Rev. Neurosci.* **23**, 155–184 (2000).
31. J. R. McReynolds *et al.*, Memory-enhancing corticosterone treatment increases amygdala norepinephrine and Arc protein expression in hippocampal synaptic fractions. *Neurobiol. Learn. Memory* **93**, 312–321 (2010).
32. C. B. Young *et al.*, Dynamic shifts in large-scale brain network balance as a function of arousal. *J. Neurosci.* **37**, 281–290 (2017).
33. E. J. Hermans *et al.*, Stress-Related Noradrenergic Activity Prompts Large-Scale Neural Network Reconfiguration. *Science* **334**, 1151–1153 (2011).
34. A. Fornito, B. J. Harrison, A. Zalesky, J. S. Simons, Competitive and cooperative dynamics of large-scale brain functional networks supporting recollection. *Proc. Natl. Acad. Sci. U.S.A.* **109**, 12788–12793 (2012).
35. K. L. Ray *et al.*, Dynamic reorganization of the frontal parietal network during cognitive control and episodic memory. *Cogn., Affective, Behav. Neurosci.* **20**, 76–90 (2020).
36. B. S. McEwen, Allostasis and allostatic load: Implications for neuropsychopharmacology. *Neuropsychopharmacology* **22**, 108–124 (2000).
37. J. M. Shine *et al.*, Computational models link cellular mechanisms of neuromodulation to large-scale neural dynamics. *Nat. Neurosci.* **24**, 765–776 (2021).
38. B. R. Munn, E. J. Müller, G. Wainstein, J. M. Shine, The ascending arousal system shapes neural dynamics to mediate awareness of cognitive states. *Nat. Commun.* **12**, 6016 (2021).
39. E. J. Hermans, M. J. A. G. Henckens, M. Joëls, G. Fernández, Dynamic adaptation of large-scale brain networks in response to acute stressors. *Trends Neurosci.* **37**, 304–314 (2014).
40. J. M. Shine, M. J. Aburn, M. Breakspear, R. A. Poldrack, The modulation of neural gain facilitates a transition between functional segregation and integration in the brain. *eLife* **7**, e31130 (2018).
41. J. M. Shine *et al.*, Human cognition involves the dynamic integration of neural activity and neuromodulatory systems. *Nat. Neurosci.* **22**, 289–296 (2019).
42. M. Mather, D. Clewett, M. Sakaki, C. W. Harley, Norepinephrine ignites local hotspots of neuronal excitation: How arousal amplifies selectivity in perception and memory. *Behav. Brain Sci.* **39**, e200 (2016).
43. E. J. Cornblath *et al.*, Temporal sequences of brain activity at rest are constrained by white matter structure and modulated by cognitive demands. *Commun. Biol.* **3**, 261 (2020).
44. J. N. v. d. Meer, M. Breakspear, L. J. Chang, S. Sonkusare, L. Cocchi, Movie viewing elicits rich and reliable brain state dynamics. *Nat. Commun.* **11**, 5004 (2020).
45. A. B. A. Stevner *et al.*, Discovery of key whole-brain transitions and dynamics during human wakefulness and non-REM sleep. *Nat. Commun.* **10**, 1035 (2019).
46. D. Vidaurre, S. M. Smith, M. W. Woolrich, Brain network dynamics are hierarchically organized in time. *Proc. Natl. Acad. Sci. U.S.A.* **114**, 12827 (2017).
47. J. P. Crutchfield, Between order and chaos. *Nat. Phys.* **8**, 17–24 (2012).
48. W. Clawson *et al.*, Computing hubs in the hippocampus and cortex. *Sci. Adv.* **5**, eaax4843 (2019).
49. T. Stalder *et al.*, Assessment of the cortisol awakening response: Expert consensus guidelines. *Psychoneuroendocrinology* **63**, 414–432 (2016).
50. M. J. Henckens, G. A. van Wingen, M. Joëls, G. Fernández, Time-dependent effects of cortisol on selective attention and emotional interference: a functional MRI study. *Front. Integrat. Neurosci.* **6**, 66 (2012).
51. T. Tian *et al.*, Socioeconomic disparities affect children's amygdala–prefrontal circuitry via stress hormone response. *Biol. Psychiatry* **90**, 173–181 (2021).
52. J. E. Pierce, J. Péron, The basal ganglia and the cerebellum in human emotion. *Soc. Cogn. Affective Neurosci.* **15**, 599–613 (2020).
53. J. H. Morrison, S. L. Foote, D. O'Connor, F. E. Bloom, Laminar, tangential and regional organization of the noradrenergic innervation of monkey cortex: Dopamine-β-hydroxylase immunohistochemistry. *Brain Res. Bull.* **9**, 309–319 (1982).
54. S. L. Foote, J. H. Morrison, Extrathalamic modulation of cortical function. *Annu. Rev. Neurosci.* **10**, 67–95 (1987).
55. M. D. Fox *et al.*, The human brain is intrinsically organized into dynamic, anticorrelated functional networks. *Proc. Natl. Acad. Sci. U.S.A.* **102**, 9673 (2005).
56. E. A. Phelps, J. E. LeDoux, Contributions of the amygdala to emotion processing: From animal models to human behavior. *Neuron* **48**, 175–187 (2005).
57. S. Heinzel *et al.*, Working memory load-dependent brain response predicts behavioral training gains in older adults. *J. Neurosci.* **34**, 1224–1233 (2014).
58. D. Barulli, Y. Stern, Efficiency, capacity, compensation, maintenance, plasticity: Emerging concepts in cognitive reserve. *Trends Cogn. Sci.* **17**, 502–509 (2013).
59. K. K. Anstrom, D. J. Woodward, Restraint increases dopaminergic burst firing in awake rats. *Neuropsychopharmacology* **30**, 1832–1840 (2005).
60. M. Joëls, R. A. Sarabdjitsingh, H. Karst, Unraveling the time domains of corticosteroid hormone influences on brain activity: Rapid, slow, and chronic modes. *Pharmacol. Rev.* **64**, 901–938 (2012).
61. D. S. Goldstein, B. McEwen, Allostasis, homeostats, and the nature of stress. *Stress* **5**, 55–58 (2002).
62. J. C. Pruessner, C. Kirschbaum, G. Meinlschmid, D. H. Hellhammer, Two formulas for computation of the area under the curve represent measures of total hormone concentration versus time-dependent change. *Psychoneuroendocrinology* **28**, 916–931 (2003).
63. A. M. Dierolf *et al.*, Effects of basal and acute cortisol on cognitive flexibility in an emotional task switching paradigm in men. *Horm. Behav.* **81**, 12–19 (2016).
64. L. Parkes, B. Fulcher, M. Yücel, A. Fornito, An evaluation of the efficacy, reliability, and sensitivity of motion correction strategies for resting-state functional MRI. *NeuroImage* **171**, 415–436 (2018).
65. J. A. Thiele, J. Faskowitz, O. Sporns, K. Hilger, Multitask brain network reconfiguration is inversely associated with human intelligence. *Cereb. Cortex* **32**, 4172–4182 (2022).
66. J. C. Pruessner *et al.*, Free cortisol levels after awakening: A reliable biological marker for the assessment of adrenocortical activity. *Life Sci.* **61**, 2539–2549 (1997).
67. Q. K. Telesford *et al.*, Detection of functional brain network reconfiguration during task-driven cognitive states. *NeuroImage* **142**, 198–210 (2016).
68. K. Capouskova, M. L. Kringelbach, G. Deco, Modes of cognition: Evidence from metastable brain dynamics. *NeuroImage* **260**, 119489 (2022).
69. M. E. Raichle, The brain's default mode network. *Annu. Rev. Neurosci.* **38**, 433–447 (2015).
70. J. Taghia *et al.*, Uncovering hidden brain state dynamics that regulate performance and decision-making during cognition. *Nat. Commun.* **9**, 2505 (2018).
71. S. Ryali *et al.*, Temporal dynamics and developmental maturation of salience, default and central-executive network interactions revealed by variational bayes hidden Markov modeling. *PLoS Comput. Biol.* **12**, e1005138 (2016).
72. D. Vidaurre *et al.*, Spectrally resolved fast transient brain states in electrophysiological data. *Neuroimage* **126**, 81–95 (2016).
73. W. R. Shirer, S. Ryali, E. Rykhlevskaia, V. Menon, M. D. Greicius, Decoding subject-driven cognitive states with whole-brain connectivity patterns. *Cereb. Cortex* **22**, 158–165 (2012).
74. A. Kottaram *et al.*, Brain network dynamics in schizophrenia: Reduced dynamism of the default mode network. *Hum. Brain Mapp.* **40**, 2212–2228 (2019).
75. L. Van der Maaten, G. Hinton, Visualizing data using t-SNE. *J. Mach. Learn. Res.* **9**, 2579–2605 (2008).
76. M. Bijanzadeh *et al.*, Decoding naturalistic affective behaviour from spectro-spatial features in multiday human iEEG. *Nat. Hum. Behav.* **6**, 823–836 (2022), 10.1038/s41562-022-01310-0.
77. V. Satopaa, J. Albrecht, D. Irwin, B. Raghavan, "Finding a "Kneedle" in a haystack: Detecting knee points in system behavior" in *2011 31st International Conference on Distributed Computing Systems Workshops* (2011), pp. 166–171.
78. T. Yarkoni, R. A. Poldrack, T. E. Nichols, D. C. Van Essen, T. D. Wager, Large-scale automated synthesis of human functional neuroimaging data. *Nat. Methods* **8**, 665–670 (2011).
79. A. Zalesky, A. Fornito, E. T. Bullmore, "Network-based statistic: Identifying differences in brain networks." *Neuroimage* **53**, 1197–1207 (2010).
80. Y. Zeng *et al.*, Cortisol awakening response prompts dynamic reconfiguration of brain networks in emotional and executive functioning. GitHub. https://github.com/QinBrainLab/2024_CAR_BrainNetwork. Deposited 27 October 2024.

Downloaded from https://www.pnas.org by HEFEI UNIVERSITY OF TECHNOLOGY on December 16, 2024 from IP address 114.213.251.57.